Sodium Tanshinone IIA Sulfonate Inhibits Canonical Transient Receptor Potential Expression in Pulmonary Arterial Smooth Muscle from Pulmonary Hypertensive Rats

Jian Wang[1,2]*, Qian Jiang[1]*, Limei Wan[1]*, Kai Yang[1,2], Yi Zhang[1,2], Yuqin Chen[1], Elizabeth Wang[3], Ning Lai[1,2], Lei Zhao[1], Hua Jiang[1], Yueqian Sun[4], Nanshan Zhong[1], Pixin Ran[1], and Wenju Lu[1]

[1]Guangzhou Institute of Respiratory Disease, State Key Laboratory of Respiratory Diseases, The 1st Affiliated Hospital of Guangzhou Medical University, China; [2]Division of Pulmonary & Critical Care Medicine, Johns Hopkins Medical Institutions, Baltimore, Maryland; [3]Department of Medicine, University of Maryland School of Medicine, Baltimore, Maryland; and [4]Department of Arts and Science, University of Toronto, Toronto, Ontario, Canada

Danshen, the dried root of *Salvia miltiorrhiza*, is widely used in clinics in China for treating various diseases, including cardiovascular diseases. Sodium tanshinone IIA sulfonate (STS), a water-soluble derivative of tanshinone IIA isolated as the major active component from Danshen, was recently reported to be effective in attenuating the characteristic pulmonary vascular changes associated with chronically hypoxic pulmonary hypertension (CHPH); however, the underlying detailed mechanisms are poorly understood. In this study, we investigated the effects of STS on basal intracellular Ca^{2+} concentration ($[Ca^{2+}]_i$) and store-operated Ca^{2+} entry (SOCE) in distal pulmonary arterial smooth muscle cells (PASMCs) exposed to prolonged hypoxia or isolated from CHPH rats. SOCE measured by Mn^{2+} quenching of Fura-2 fluorescence in PASMCs from rats exposed to chronic hypoxia (10% O_2, 21 d) was increased by 59%, and basal $[Ca^{2+}]_i$ was increased by 119%; this effect was inhibited by intraperitoneal injection of STS. These inhibitory effects of STS on hypoxic increases of SOCE and basal $[Ca^{2+}]_i$ were associated with reduced expression of canonical transient receptor potential (TRPC)1 and TRPC6 in distal pulmonary arterial smooth muscle and decreases on right ventricular pressure, right ventricular hypertrophy, and peripheral pulmonary vessel thickening. In *ex vivo* cultured distal PASMCs from normoxic rats, STS (0–25 μM) dose-dependently inhibited hypoxia-induced cell proliferation and migration, paralleled with attenuation in increases of basal $[Ca^{2+}]_i$, SOCE, mRNA, and protein expression of TRPC1 and TRPC6. STS also relieved right ventricular systolic pressure, right ventricular hypertrophy, and TRPC1 and TRPC6 protein expression in distal pulmonary arteries in a monocrotaline-induced rat model of pulmonary arterial hypertension. These results indicate that STS prevents pulmonary arterial hypertension development likely by inhibiting TRPC1 and TRPC6 expression, resulting in normalized basal $[Ca^{2+}]_i$ and attenuated proliferation and migration of PASMCs.

CLINICAL RELEVANCE

The widespread application of treatments for pulmonary hypertension is hindered by their huge costs and limited efficacy. Sodium tanshinone IIA sulfonate (STS), a Chinese traditional medicine that is widely used in China, is indicated to be able to prevent chronically hypoxic pulmonary hypertension development. Due to its low cost and few side effects, STS is a valuable candidate deserving further investigation for future hypoxic pulmonary hypertension therapy.

Keywords: STS; TRPC; SOCE; pulmonary hypertension

Pulmonary arterial hypertension (PAH) is a rare yet life-threatening disease that affects 15 per 1 million adults, according to the most recent estimation in 2008 (1). It is physiologically defined by mean pulmonary arterial pressure of 25 mm Hg or greater at rest and is pathologically characterized by pulmonary vascular remodeling, including smooth muscle hypertrophy and intima thickening. Although significant progress has been made in the past decades in our understanding of PAH and in disease management, the prognosis is still poor, with a 1-year survival rate of 91.0% (2) and 3-year survival rate of 77% or less according to recent investigations (3–5). The principal treatments for PAH rely on approaches targeting the prostacyclin, endothelin, or NO pathways (phosphodiesterase inhibition) or, increasingly, on a combination of them (6–11). Few patients show indication for treatment with calcium channel blockers. However, their high costs and limited efficacy have hindered their widespread clinical application.

Sodium tanshinone IIA sulfonate (STS) is a water-soluble derivative of tanshinone IIA isolated as the main pharmacologically active component from a traditional Chinese herbal medicine, the dried root of *Salvia miltiorrhiza* known as Danshen. Danshen has long been extensively used in improving body functions,

(*Received in original form February 22, 2012 and in final form September 19, 2012*)

* These authors contributed equally to this work.

This work was supported by National Institutes of Health grant R01HL093020; National Natural Science Foundation of China grants 81070043, 81071917, 81173112, and 81170052; Chinese Central Government Key Research Projects of the 973 grant 2009CB522107; Changjiang Scholars and Innovative Research Team in University grant IRT0961; Guangdong Department of Science and Technology of China grants 2009B050700041 and 2010B03160030;, Guangdong Province Universities and Colleges Pearl River Scholar Funded Scheme (2008) China; Guangdong Natural Science Foundation Team grant 1035101200300000; Guangdong Department of Education Research grant cxzd1025; Guangzhou Department of Education Yangcheng Scholarship (10A058S); and Guangzhou Department of Science and Technology, China grant 2010J-E181.

Author Contributions: J.W. initiated the project, designed the experiments, analyzed the data, and drafted and revised the paper. Q.J. and L.W. contributed to the animal, functional, and molecular experiments. Y.Z., K.Y., N.L., and Y.S. contributed to the cellular and molecular experiments. Y.C. contributed to the animal and functional experiments. E.W., L.Z., and H.J. contributed to the functional experiments and manuscript editing. N.Z. and P.R. consulted on the design of the paper. W.L. initiated the project, designed the experiments, analyzed the data, and wrote and revised the paper.

Correspondence and requests for reprints should be addressed to Wenju Lu, Ph.D. Guangzhou Institute of Respiratory Diseases, State Key Laboratory of Respiratory Diseases, The First Affiliated Hospital, Guangzhou Medical University, 151 Yanjiang Road, Guangzhou, Guangdong, 510120, People's Republic of China. E-mail: wlu92@yahoo.com

This article has an online supplement, which is accessible from this issue's table of contents at www.atsjournals.org

Am J Respir Cell Mol Biol Vol 48, Iss. 1, pp 125–134, Jan 2013

Originally Published in Press as DOI: 10.1165/rcmb.2012-0071OC on October 11, 2012
Internet address: www.atsjournals.org

such as promoting circulation and improving blood flow (12, 13). Danshen and its various formula products in numerous pharmaceutical dosage forms are commercially available and are commonly administered to treat inflammatory and cardiovascular diseases in the clinics in China with negligible adverse effects (14–17). STS has been clinically used in Asian countries for the prevention and treatment of coronary heart disease (18). Recent studies indicated that STS exerts protective effects on hypoxic pulmonary hypertension, including lowering pulmonary artery pressure and decreasing pulmonary artery thickness and right ventricular hypertrophy (19). These effects were suggested to be achieved partially through the regulation of intracellular Ca^{2+} homeostasis in pulmonary arterial smooth cells (PASMCs) (19, 20); however, the underlying detailed mechanisms remain largely unclear and deserve further investigation. The elucidation of the involved mechanisms will serve as a rationale for the potential clinical application of STS or tanshinone IIA in PAH treatment, which could benefit thousands of patients with PAH by greatly reducing their medical expenses.

Among numerous mechanisms that have been identified as influencing the development of PAH, hypoxia is thought to be a pivotal factor triggering pulmonary vascular contraction (21) and remodeling (22). Animals such as rat and mouse exposed to chronic hypoxia developed chronically hypoxia pulmonary hypertension (CHPH) in less than 3 weeks (23–25). In PASMCs, elevation of intracellular Ca^{2+} concentration ($[Ca^{2+}]_i$) via Ca^{2+} influx through store-operated Ca^{2+} channels (SOCC) thought to be composed of canonical transient receptor potential (TRPC) proteins is an important determinant of cell growth and contraction (26–29). We previously demonstrated that chronic hypoxia elevated basal $[Ca^{2+}]_i$ in PASMCs due in large part to enhanced store-operated Ca^{2+} entry (SOCE); moreover, *ex vivo* exposure to prolonged hypoxia up-regulated TRPC1 and TRPC6 expression in PASMCs (27, 29–31). A monocrotaline (MCT)-induced PH animal model is also commonly used to study the pathological mechanisms of PAH. In the present study, we confirmed the suppressive effects of STS on PAH development in two independent animal models: CHPH and MCT-induced PH. We also examined the effects of STS on increases of TRPC expression, SOCE, and basal $[Ca^{2+}]_i$ levels in PASMCs resulting from chronically hypoxia, aiming to elucidate the pharmacological mechanisms of how STS prevents CHPH development.

MATERIALS AND METHODS

CHPH and MCT-Induced PAH Rat Model Establishment and STS Treatment

All procedures were approved by the Animal Care and Use Committee of Guangzhou Medical University. For CHPH model establishment, adult male Sprague-Dawley rats (175–300 g) were put in a hypoxic chamber for 21 days as previously described (29, 32). In this model, four groups of animals were examined: normoxic control, normoxia+STS, hypoxic control, and hypoxia+STS. In experiments with the MCT-induced PAH model, rats were given a single subcutaneous injection of 50 mg/kg MCT (Sigma-Aldrich, St. Louis, MO) or saline, and then the animals were randomly grouped as saline control, MCT control, and MCT+STS. For both PAH models, STS (Shanghai No 1 Biochemical-Pharmaceutical Co., Ltd, Shanghai, China) was given to the rats by intraperitoneal injection at 10 mg/kg/d for 21 days. Control groups of animals received equivalent amount of saline.

Hemodynamic Measurements and Lung Histochemistry

Right ventricular systolic pressure and right ventricular hypertrophy were measured using the same method as we described previously (30). Intrapulmonary vessels were visualized by H&E staining on formalin-fixed and paraffin-embedded lung cross-sections (5 μm thickness). Details are provided in the online supplement.

Culture and Treatments of Rat Distal PASMCs

The method for obtaining rat distal PASMCs has been described previously (25, 27). The isolated PASMCs were seeded in 6-well culture dishes and cultured in Smooth Muscle Growth Medium-2 (Clonetics, Walkersville, MD) in a humidified atmosphere of 5% CO_2 and 95% air at 37°C for 3 to 4 days. For prolonged hypoxia and STS treatment, cells were replaced with Smooth Muscle Basal Medium (Clonetics) containing 0.3% FBS for 24 hours to reach a growth arrest before being exposed to hypoxia (4% O_2) or normoxia in the presence or absence of STS for 60 hours before various assessments. The O_2 concentration in the culture media was continuously monitored in real time using an O_2 sensor (8-730 flow-through O_2 microelectrodes; Microelectrodes Inc., Bedford, NH). This demonstrated that the level of O_2 dropped to 6% at approximately 6 hours and reached 4% at approximately 16 hours after hypoxia exposure (4% O_2) (*see* Figure E1A in the online supplement). The cells isolated from CHPH animals were transiently cultured in Ham's F-12 medium with L-glutamine (Mediatech Inc., Manassas, VA) supplemented with 0.5% FBS for 24 to approximately 48 hours before $[Ca^{2+}]_i$ measurement.

Cell Proliferation and Cytotoxicity Assessment

PASMC proliferation was assessed using an Amersham Cell Proliferation Biotrak ELISA kit (GEhealthcare, Buckinghamshire, UK). Cytotoxicity of various doses of STS (0–25 μM) on PASMCs was analyzed using CytoTox-Glo Cytotoxicity Assay kit (Promega, Madison, WI). Cell viability was calculated as percentage ratios of luminescence for viable cells to total per treatment well. Details are provided in the online supplement.

Cell Migration Assay

PASMCs treated with 0 to approximately 25 μM STS for 60 hours under normoxic or hypoxic conditions were loaded on the 8-μm polycarbonate membrane of Transwell Permeable Support (24 mm) (Corning Inc., Corning, NY) (1×10^5 cells per well) and cultured in Smooth Muscle Basal Medium containing 0.3% FBS for 24 hours. Cells on the membrane were stained with Brilliant Blue R and counted to calculate the migration rate. Details are provided in the online supplement.

Intracellular Ca^{2+} Determination

SOCE was measured in PASMCs using Fura-2 dye and fluorescent microscopy as previously described (27, 29). To obtain statistically convincing results, the fluorescence intensity was determined in at least 20 cells for each sample. Details are provided in the online supplement.

Quantitative RT-PCR

Total RNA was extracted using the TRIzol method for deendothelialized distal PA or using the RNeasy kit (Qiagen, Valencia, CA) for PASMCs as previously described (27, 29, 31). Reverse transcription and real-time PCR were performed as described previously (30, 33, 34). Details are provided in the online supplement.

Western Blotting

Rat distal PA or PASMCs were sonicated or lysed in TPER lysis buffer (Pierce, Rockford, IL) with a protease inhibitor cocktail tablet, and protein expression was measured by immunoblotting assay as described previously (27, 29, 33). Details are provided in the online supplement.

Statistical Analysis

Statistical analyses were conducted using one-way ANOVA for multiple and Student's *t* test for two data groups. All data in this study were tested and found fit for normal distribution. When F ratios obtained with ANOVA were significant, Fisher's protected least significant difference was used for pairwise comparisons of means. Differences were considered significant when $P < 0.05$. Data are presented as means ± SEM; "*n*" refers to the sample size, (i.e., the number of the animals providing pulmonary arteries or primary culture of PASMCs).

RESULTS

STS Inhibited the Characteristic Changes of CHPH in Rats

Consistent with our previous results (29, 33), rats exposed to chronic hypoxia (10% O_2 for 21 d) developed CHPH. Right ventricular systolic pressure (RVSP) was increased from 24.7 ± 0.64 mm Hg in normoxic control rats to 60.1 ± 2.75 mm Hg in hypoxic control rats (Figures 1A and 1B). The development of CHPH was accompanied by right ventricular hypertrophy, indicated by the increases on weight ratio of right ventricle (RV) to left ventricle (LV) plus septum (RV/LV+S) from 0.26 ± 0.035 (normoxia) to 0.55 ± 0.042 (hypoxia; $P < 0.001$ versus normoxia) (Figure 1C) and increases on the ratio of right ventricle to body weight (RV/body weight) from 0.46 ± 0.01 (normoxia) to 1.09 ± 0.07 (hypoxia; $P < 0.001$ versus normoxia) (Figure 1D). Injection of STS (10 mg/kg/d) significantly reduced these characteristic changes of CHPH. Accordingly, STS caused a significant decrease of mean RVSP to 48.7 ± 1.95 mm Hg (hypoxia + STS) ($P < 0.001$ versus hypoxia control) (Figures 1A and 1B), RV/(LV+S) to 0.42 ± 0.03 mm Hg ($P < 0.001$ versus hypoxia control) (Figure 1C), and RV/body weight ratios to 0.88 ± 0.02 ($P < 0.05$ versus hypoxia control) (Figure 1D) in chronically hypoxic rats. STS did not affect the

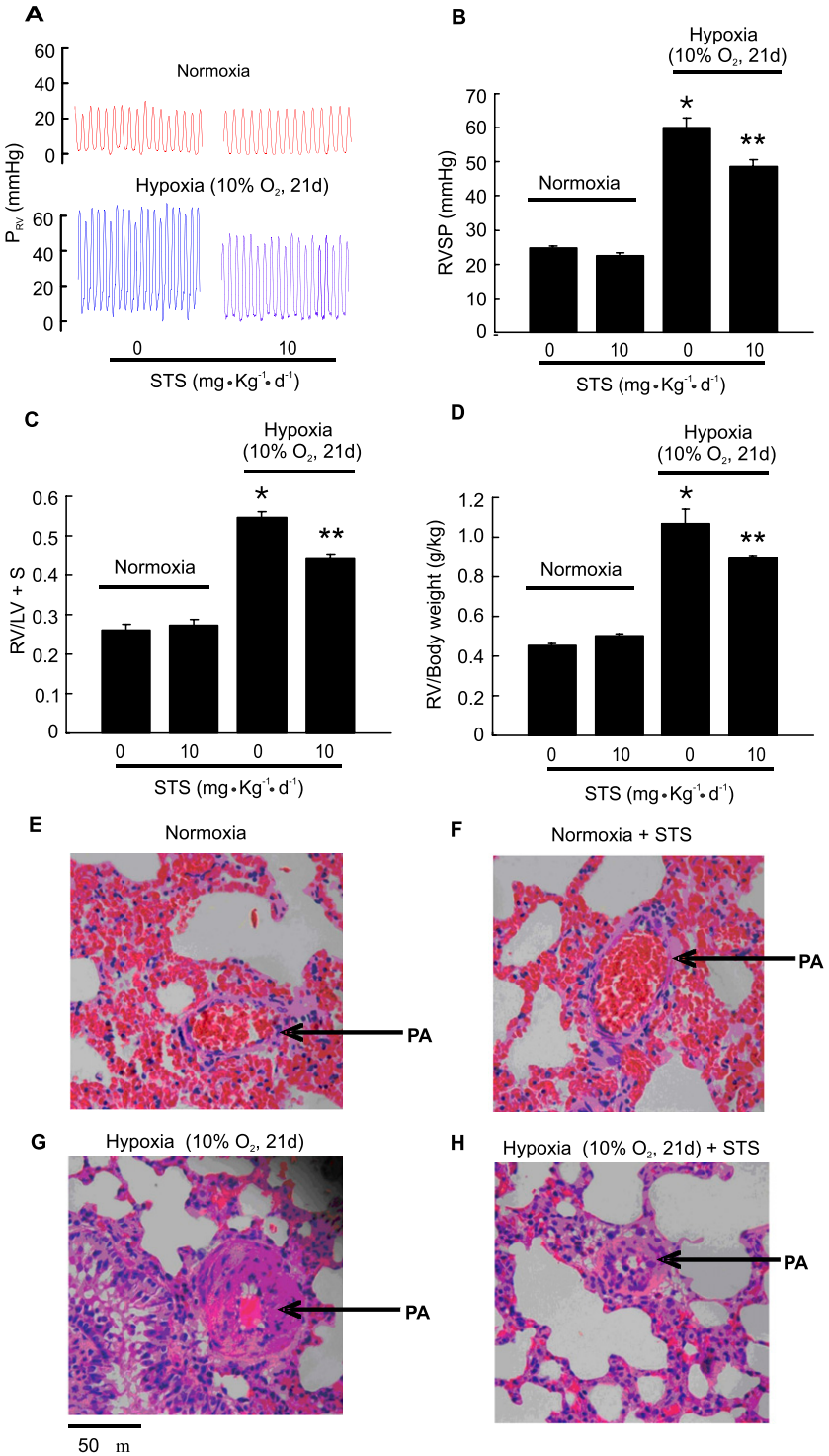

Figure 1. Effects of sodium tanshinone IIA sulfonate (STS) on hemodynamic parameters of chronically hypoxic pulmonary hypertension (CHPH) and pulmonary vascular remodeling in rats. Animals were exposed to normoxia or hypoxia (10% O_2) for 21 days with or without STS (intraperitoneally, 10 mg/kg/d) treatment. (*A*) Representative traces of right ventricular systolic pressure (RVSP) of each group of animals. (*B–D*) Bar graphs showing RVSP, right ventricular (RV)/left ventricular (LV)+S, and RV/body weight, respectively. Bar values are means ± SEM ($n = 7$ in each group). *$P < 0.01$ versus respective normoxic control. **$P < 0.01$ versus respective hypoxic control. (*E–H*) Lung tissues were fixed in neutral buffered formalin, embedded in paraffin, cross-sectioned (5 μM in thickness), and stained with hematoxylin and eosin. Pictures are representative from four for each group of animals treated with normoxia (*E*), normoxia + STS (*F*), hypoxia (*G*), or hypoxia + STS (*H*), showing an inhibitory role of STS on pulmonary artery wall thickening induced by hypoxia. *Arrows* indicate pulmonary artery in each picture. P_{RV} = Right ventricular pressure.

mean RVSP (23.1 ± 1.1 mm Hg; $P = 0.32$) (Figures 1A and 1B), the RV/(LV+) ratio (0.27 ± 0.016; $P = 0.55$) (Figure 1C), or the RV/body weight ratio (Figure 1D) in normoxic animals, with P values being calculated by comparing the normoxic STS group with the normoxic control group.

The animals were weighed every 3 days during the 21-day hypoxia exposure. Consistent with what we observed previously (35), the hypoxic control rats initially displayed approximately 1.1% body weight loss when weighed at Day 3 of hypoxia exposure; however, these animals displayed body weight gain during the further period of study. All normoxic control animals increased their body weight throughout the study. Treatment with STS did not cause body weight change under normoxic or hypoxic conditions (data not shown). At the end of the experiment at Day 21 of hypoxia exposure and STS treatment, the weight ratios ($\times 10^{-2}$) of liver to whole body and kidney to whole body were not changed by hypoxia exposure or STS treatment (data not shown), indicating good tolerance to these treatments.

Histochemistry examinations demonstrated that the distal pulmonary arterial walls, especially the tunica media, were greatly thickened in the hypoxic control rats (Figure 1H) that developed CHPH when compared with those from normoxic control animals (Figure 1F). STS relieved the hypoxia-induced pulmonary arterial wall thickening (Figure 1I) without affecting those in normoxic rats (Figure 1G).

STS Attenuated the Increases of SOCE and Basal $[Ca^{2+}]_i$ in Distal PASMCs from Chronically Hypoxic Rats

PASMCs were isolated from rats exposed to chronic hypoxia with or without STS. SOCE was assessed by Mn^{2+} fluorescence quenching and was represented as the percent decrease in fluorescence intensity in 10 minutes. In rats without STS injection, Mn^{2+} quenching was significantly enhanced in PASMCs from hypoxic control animals (35.4 ± 3.6% for normoxia versus 56.3 ± 5.2% for hypoxia; $P < 0.05$; $n = 4$ for each group) (Figures 2A and 2B), and basal $[Ca^{2+}]_i$ was increased from 115.3 ± 16.6 nM in normoxic cells to 252.5 ± 27.6 nM in hypoxic PASMCs ($P < 0.05$; $n = 5$ in each group). STS administration (10 mg/kg/d) reduced the hypoxic increases of Mn^{2+} quenching (43.5 ± 3.6% for STS treated hypoxic cells; $n = 4$; $P < 0.05$ versus hypoxic control cells). Moreover, STS inhibited the hypoxic elevation of basal $[Ca^{2+}]_i$ in PASMCs from chronically hypoxic rats (149.0 ± 26.1 nM; $n = 5$; $P < 0.05$ compared with hypoxic control) (Figure 2C). STS treatment did not influence SOCE (Figures 2A and 2B) or basal $[Ca^{2+}]_i$ (Figure 2C) in PASMCs from normoxic control rats.

STS Inhibited the Hypoxic Up-Regulation of TRPC1 and TRPC6 Expression in Rat Distal PA

Similar to our previous observations (29), mRNA and protein expressions of TRPC1 (Figures 3A and 3C) and TRPC6 (Figures

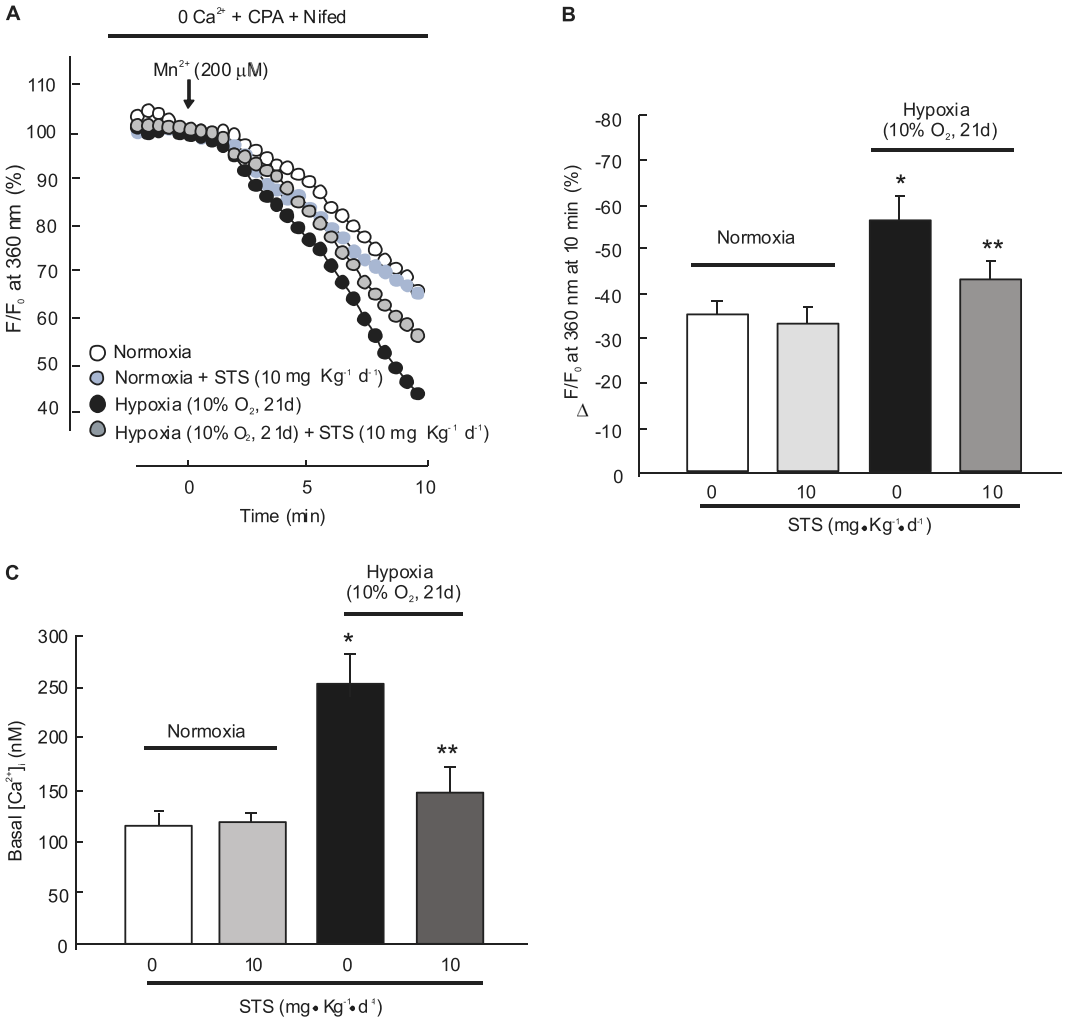

Figure 2. Effects of STS on store-operated Ca^{2+} entry (SOCE) and basal intracellular Ca^{2+} concentration ($[Ca^{2+}]_i$) in pulmonary arterial smooth muscle cells (PASMCs) isolated from rats exposed to hypoxia. PASMCs were isolated from normoxic or hypoxic (10% O_2 for 21 d) rats with or without STS (10 mg/kg/d) treatment. (*A*) SOCE determined by measuring the time course of Fura-2 fluorescence intensity excited at 360 nm before and after adding 200 μM Mn^{2+} in Ca^{2+}–free Krebs-Ringer bicarbonate solution (0 Ca^{2+}) perfusate containing 10 μM cyclopiazonic acid (CPA) and 5 μM nifedipine (Nifed) in PASMCs. Data at each time point were normalized to fluorescence at time 0 (F/F_0). (*B*) Average quenching of Fura-2 fluorescence by Mn^{2+}. Data are expressed as the percentage decrease in fluorescence at time 10 minutes from time 0. The tested cell numbers in each group were as below: normoxia (115 cells; $n = 4$), normoxia+STS (117 cells; $n = 4$), hypoxia (118 cells; $n = 4$), and hypoxia+STS (117 cells; $n = 4$). Bar values are mean ± SEM. *$P < 0.05$ versus normoxic control. **$P < 0.05$ versus hypoxic control. (*C*) Basal $[Ca^{2+}]_i$ in PASMCs from rats treated with normoxia, normoxia+STS, hypoxia, or hypoxia+STS. Bar values are means ± SEM ($n = 5$ in each group). *$P < 0.05$ versus normoxic control. **$P < 0.05$ versus hypoxic control.

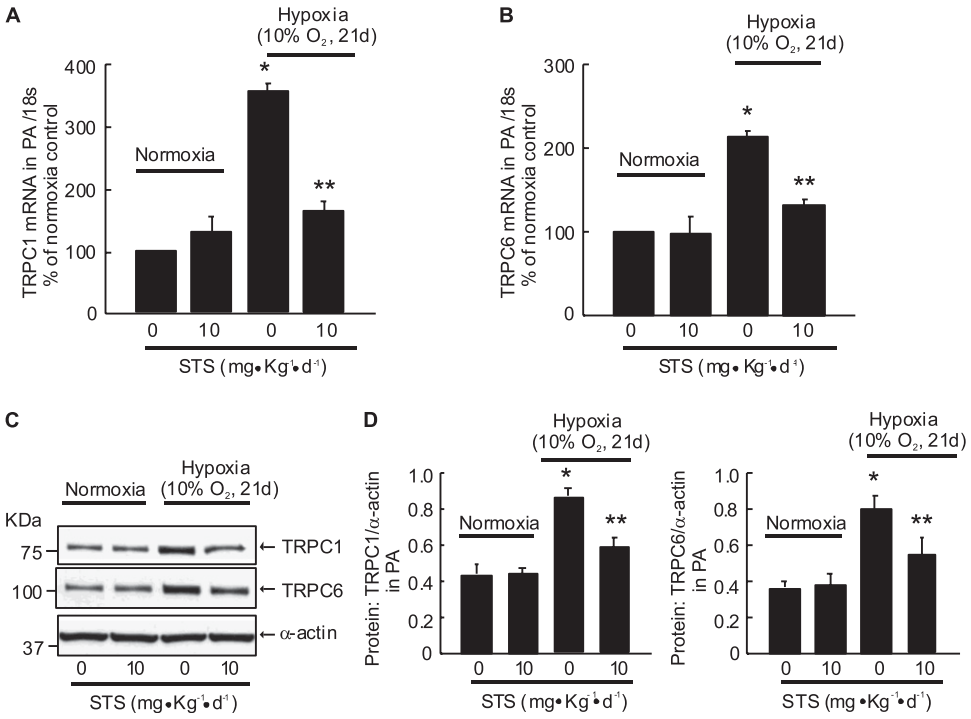

Figure 3. Effect of STS (intraperitoneally, 10 mg/kg/d) on canonical transient receptor potential (TRPC) expression in distal PA from rats exposed to normoxia or hypoxia (10% O_2) for 21 days. TRPC1 (*A*) and TRPC6 (*B*) mRNA relative to 18 s was measured by real-time quantitative PCR. TRPC1 and TRPC6 proteins were determined by Western blotting (*C* and *D*). Representative blots (*C*) and mean intensity (*D*) for TRPC1 or TRPC6 blots relative to α-actin. Bar values are mean ± SEM ($n = 4$ in each group). *$P < 0.05$ versus respective normoxia control. **$P < 0.05$ versus respective hypoxia control.

3B and 3D) were increased in distal PA from rats exposed to chronic hypoxia (10% O_2, 21 d) compared with normoxic control animals. STS treatment (10 mg/kg/d) suppressed these hypoxia-induced increases but did not affect the levels of TRPC1 and TRPC6 in PA from normoxic rats.

Effects of STS on Hypoxia-Induced Proliferation and Migration of PASMCs

Prolonged hypoxia (4% O_2, 60 h) enhanced proliferation (Figure 4A) and migration (Figure 4B) of PASMCs; these enhancements were inhibited by STS (0.1–25 μM) in a dose-dependent manner, with significant inhibition at 12.5 and 25 μM of STS. None of the tested STS dosages affected PASMCs viability under the experimental conditions (Figure 4C), indicating that the inhibitory effects of STS on cell proliferation and migration were not due to the cytotoxic effects accumulated with concentration increases.

STS Inhibited Prolonged Hypoxia-Induced TRPC Expression in PASMCs from Normoxic Rats

Isolated PASMCs from normoxic rats were exposed to prolonged hypoxia (4% O_2, 60 h) with or without STS. Hypoxia exposure increased TRPC1 and TRPC6 mRNA expression by 60.1 and 76.3%, respectively (Figures 5A and 5B). Consistent with the alteration in mRNA levels, hypoxia exposure caused 117.3 and 124.6% increases of TRPC1 and TRPC6 protein expression, respectively. Treatment with STS (12.5 μM) blocked these hypoxic increases in mRNA and protein of TRPC1 and TRPC6 (Figures 5C and 5D). Under normoxic conditions, the expressions of TRPC1 and TRPC6 in mRNA or protein level were not changed by STS treatment (Figure 5).

Previously, we demonstrated that treatment with specific siRNA for TRPC1 (siT1) or TRPC6 (siT6) resulted in approximately 80% reduction of TRPC1 or TRPC6 protein expression in PASMCs, and the knockdown of these protein led to a significant reduction of the hypoxic increases of SOCE and basal $[Ca^{2+}]_i$ in PASMCs exposed to prolonged hypoxia (30). To further determine the causal relationship between TRPC1 and TRPC6 protein expression and the hypoxic increases of PASMC proliferation and migration, we examined the effects of siT1 and siT6 on PASMC proliferation and migration under prolonged hypoxic conditions. As seen in Figures E2A and E2B, exposure to prolonged hypoxia caused an approximately 70% increase in proliferation and a 90% increase in migration of PASMCs treated with nontargeting control siRNA; however, treatment with siT1 or siT6 decreased these hypoxic responses. These results indicate that the hypoxic up-regulation of TRPC1 and TRPC6 are responsible, at least in part, for the enhanced proliferation and migration of rat distal PASMCs under prolonged hypoxic conditions.

STS Impaired the Consequent Increases of SOCE and Basal $[Ca^{2+}]_i$ in PASMCs Exposed to Prolonged Hypoxia

Consistent with our previous findings (29), SOCE determined by Mn^{2+} quenching at 10 minutes of perfusion was higher in hypoxia-treated PASMCs (58.7 ± 3.9%; $n = 4$; $P < 0.001$ versus normoxia) (Figures 6A and 6B) than in normoxic cells (37.9 ± 2.2%; $n = 3$). STS (12.5 μM) decreased the Mn^{2+} quenching rate to approximately 78.9% in hypoxic cells (46.3 ± 3.8% in STS-treated hypoxic cells; $P < 0.05$ versus hypoxic control cells) (Figures 6A and 6B) but not in normoxic cells (37.5 ± 3.2% in STS-treated normoxic cells versus normoxic control cells; $P = 0.68$) (Figures 6A and 6B).

Basal $[Ca^{2+}]_i$ in PASMCs exposed to prolonged hypoxia (4% O_2, 60 h) was increased to 250.2 ± 71.6 nM ($P < 0.05$ compared with 144.9 ± 24.5 nM in normoxic cells) (Figure 6C), which was completely blocked by treatment with 12.5 μM STS (85.1 ± 29.3 nM; $n = 5$; $P < 0.001$ versus hypoxic control cells) (Figure 6C). Similar STS treatments did not alter basal $[Ca^{2+}]_i$ in cells under normoxic conditions (Figure 6C).

STS Inhibited the Hemodynamic Parameters of MCT-Induced PAH in Rats

MCT treatment induced PAH in rats, as indicated by elevated RVSP (74.3 ± 1.9 mm Hg; $P < 0.001$ versus 25.0 ± 0.71 mm

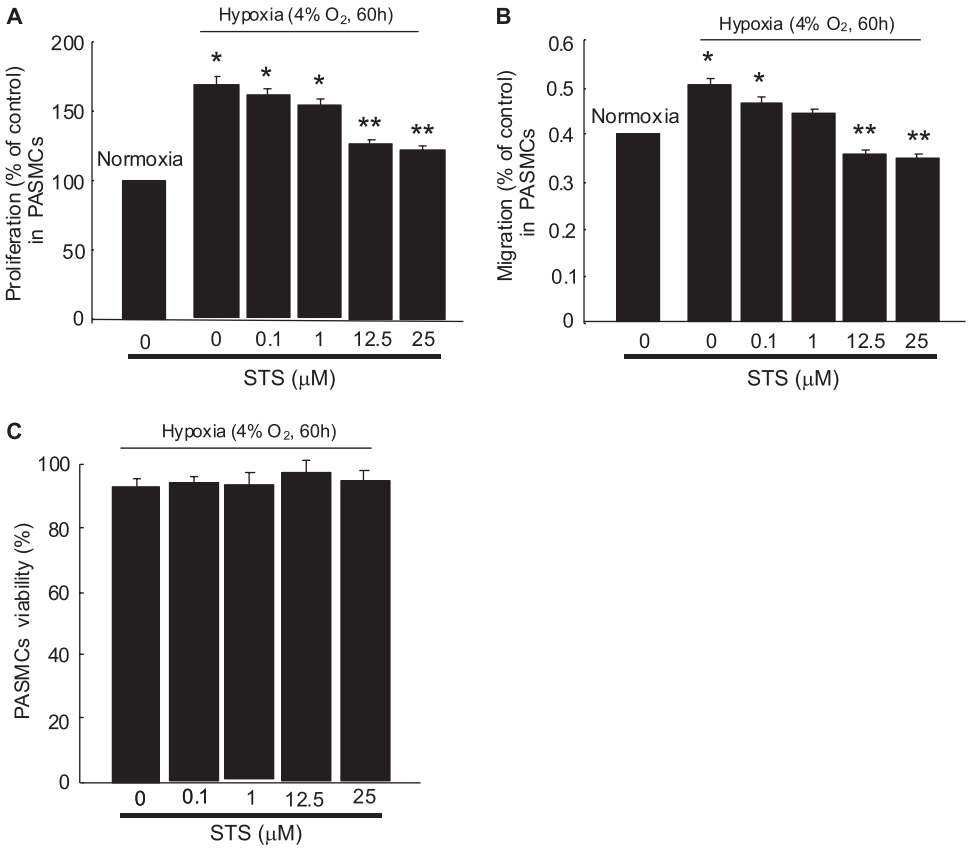

Figure 4. Effect of STS on proliferation, migration, and viability of PASMCs under prolonged hypoxia. PASMCs from normoxic rats were treated with normoxia or hypoxia (4% O_2) for 60 hours with or without STS at various dosages (0 to $\sim$ 25 μM). (*A*) Cell proliferation was assessed by analyzing the BrdU incorporation rate under normoxic or hypoxic conditions. (*B*) The migration rates of cells cultured under normoxic or hypoxic conditions were determined by calculating the ratios of migrated cells (on the lower surface of trans-well membrane) to the total cells (cells on both sides of trans-well membrane). In *A* and *B*, values were normalized to normoxia alone and presented as percentages. *$P < 0.05$ compared with normoxic control. **$P < 0.05$ compared with hypoxic control ($n = 4$ in each treatment group). (*C*) PASMC viability after various doses of STS treatment under hypoxic condition was assessed by measuring dead-cell protease activity and presented as the percentage of viable cells to total cells ($n = 3$ in each treatment group).

Hg in saline control animals) (Figures 7A and 7B) and increased the RV/(LV+S) ratio (0.62 ± 0.010; $P < 0.001$ versus 0.30 ± 0.011 in saline control animals) (Figure 7C) in MCT-treated control animals (Figure 7). Treatment with STS (10 mg/kg/d) significantly reduced the pressure increase (51.2 ± 1.64 mm Hg; $P < 0.001$ versus MCT control) (Figures 7A and 7B) and RV/(LV+S) ratio (0.47 ± 0.015; $P < 0.001$ versus MCT control) (Figure 7C) in MCT-treated rats (Figure 7A). These inhibitory effects of STS on the hemodynamic parameters of MCT-induced PAH were associated with significantly attenuated expression of TRPC1 and TRPC6 protein in the distal PA (Figures 7D and 7E).

DISCUSSION

Danshen and its derived products have been widely used to treat various cardiovascular diseases in clinics in China; however, like

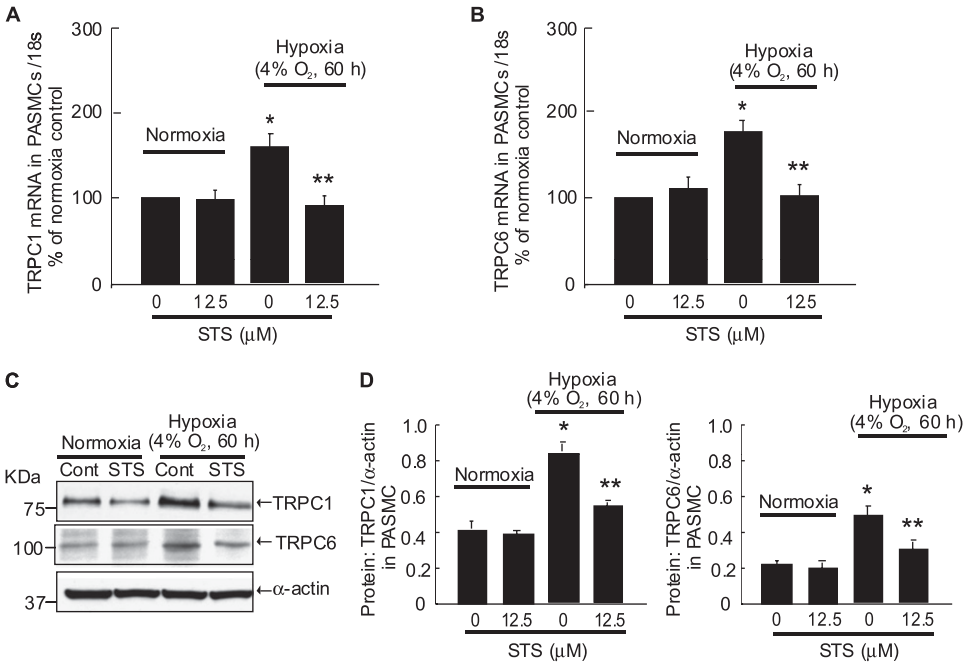

Figure 5. STS inhibited TRPC expression, SOCE, and basal $[Ca^{2+}]_i$ in PASMCs exposed to prolonged hypoxia. PASMCs isolated from normoxic rats were treated with prolonged hypoxia (4% O_2, 60 h) with or without STS (12.5 μM) treatment. The relative mRNA levels (to 18 s) for TPRC1 and TRPC6 were determined by quantitative RT-PCR, and the results are shown as percentage of that of normoxia in *A* and *B*. The protein levels of TRPC1 and TRPC6 were measured by Western blotting (*C*), and their band intensities were normalized to that of α-actin (*D*). Data are presented as means ± SEM ($n = 4$ in each group). *$P < 0.05$ versus normoxic control. **$P < 0.05$ versus hypoxic control.

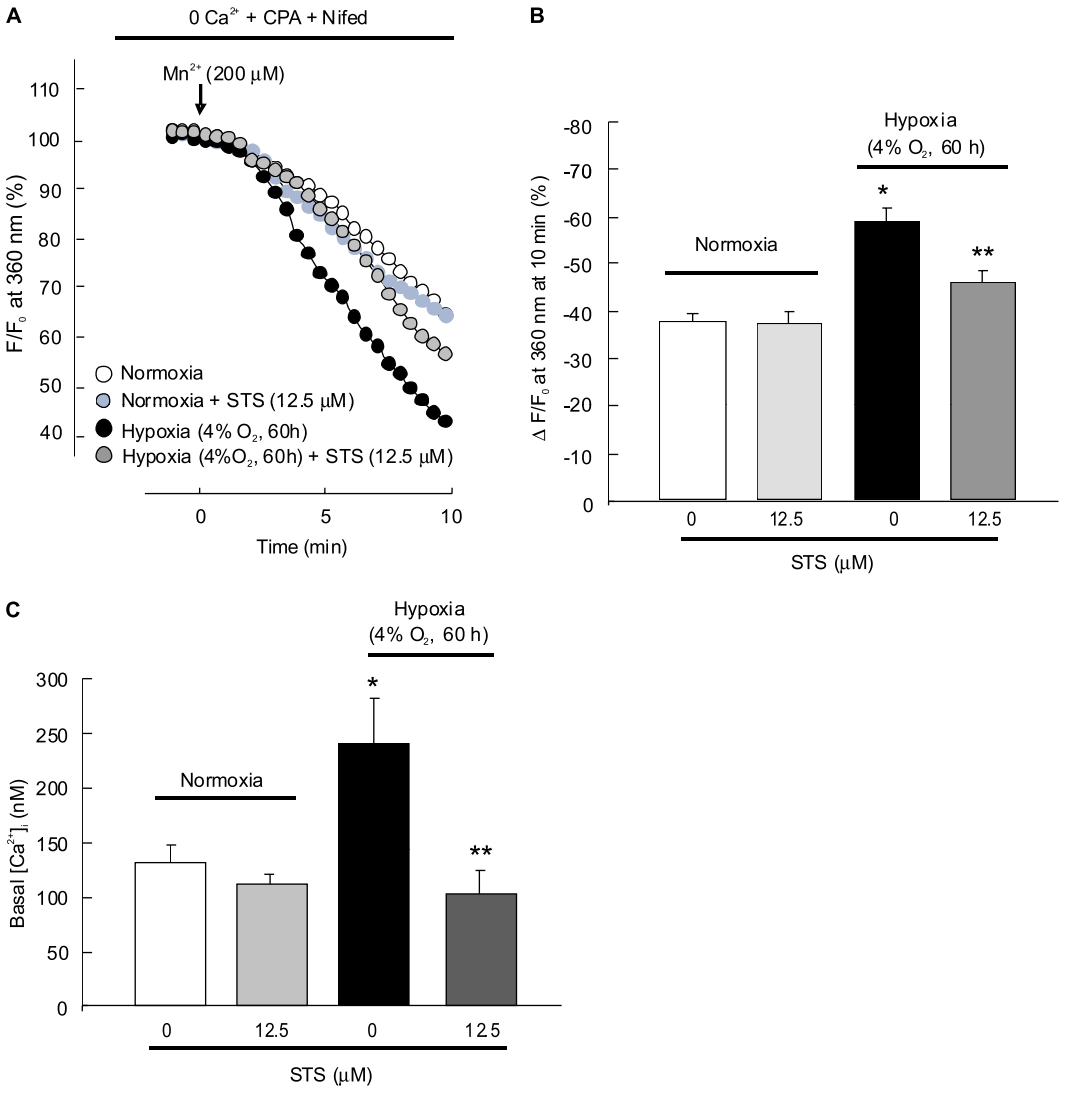

Figure 6. Effects of STS on SOCE and basal $[Ca^{2+}]_i$ in PASMCs exposed to prolonged hypoxia. PASMCs isolated from normoxic rats were treated with normoxia or hypoxia (4% O_2, 60 h) with or without STS (12.5 μM). The levels of SOCE were determined by measuring the Mn^{2+} fluorescence quenching rate. (*A*) Time course of Fura-2 fluorescence excited at 360 nm before and after adding 200 μM Mn^{2+} in Ca^{2+}–free Krebs-Ringer bicarbonate solution (0 Ca^{2+}) perfusate containing 10 μM CPA and 5 μM Nifed in PASMCs treated with normoxia ($n = 4$ in 112 cells), normoxia+STS ($n = 4$ in 110 cells), hypoxia (4% O_2; $n = 4$ in 120 cells), or hypoxia plus STS ($n = 4$ in 116 cells). Data were normalized to fluorescence at time 0 (F/F_0). (*B*) Average quenching of Fura-2 fluorescence by Mn^{2+}. Data were expressed as the percentage decrease in fluorescence at time 10 minutes from time 0; all bar values are mean ± SEM. *$P < 0.05$ versus normoxic control. **$P < 0.05$ versus hypoxic control. (*C*) Basal $[Ca^{2+}]_i$ in PASMCs treated with normoxic control ($n = 5$ experiments from 149 cells), normoxia+STS ($n = 5$ experiments from 145 cells), hypoxic control (4% O_2; $n = 5$ experiments from 148 cells), or hypoxia+STS ($n = 5$ experiments from 146 cells) for 60 hours. Bar values are mean ± SEM. *$P < 0.001$ versus normoxic control. **$P < 0.01$ versus hypoxic control.

most other traditional Chinese medicines, the pharmacological molecular targets of these treatments are unknown. Our studies provided fundamental mechanistic evidence that treatment with STS inhibited increases of TRPC1 and TRPC6 in CHPH animals associated with ameliorated CHPH symptoms and decreased SOCE and basal $[Ca^{2+}]_i$ in PASMCs. These results suggest that STS could be potentially used to treat PAH through its effects on regulating intracellular Ca^{2+} homeostasis in PASMCs.

We confirmed that intraperitoneal injection with STS attenuated pulmonary vascular resistance and remodeling in a rat CHPH model, which was indicated by decreased RV systolic pressure, RV hypertrophy, and medial wall thickening of small pulmonary vasculature. These results are consistent with previous reports (19). The dose of STS (10 mg/kg/d) used here to treat CHPH did not cause a detectable toxic effect, as evaluated by parameters including organ and body index. The inhibitory effect of STS on right ventricular hypertrophy could be subjected to the reduction of RVSP; it is also likely that this effect was due to the direct inhibition of STS on cardiac myocyte hypertrophy induced by angiotension II, a known pathological factor that is elevated during CHPH and thought to contribute to pulmonary vascular remodeling and right ventricular hypertrophy (15, 36, 37). STS has been shown to protect myocytes against apoptosis, inhibit NAD(P)H oxidase activity, and promote VEGF expression and angiogenesis in myocardial tissue and thus improve cardiac function in experimental diabetic, hypertensive, and myocardial ischemia injury rats (38–40). Under the disease condition of CHPH, the exact action of STS on right ventricular hypertrophy and heart function needs further investigation.

Because we previously showed that PASMCs isolated from CHPH rats exhibited elevated $[Ca^{2+}]_i$ and because $[Ca^{2+}]_i$ has been reported to be an important determinant in modulating PASMC contraction, proliferation, and growth associated with vasoconstriction and pulmonary vascular remodeling (41–44), it is reasonable to assume that the effects of STS on attenuating CHPH development were achieved through inhibiting basal $[Ca^{2+}]_i$. As a result of this study, we found that PASMCs from chronic hypoxia–exposed rats displayed significantly increased basal $[Ca^{2+}]_i$ and enhanced SOCE, which were almost completely abolished by STS treatment.

In vascular smooth muscle cells, increases of $[Ca^{2+}]_i$ can be caused by Ca^{2+} release from internal storage sites, such as sarcoplasmic reticulum, and by Ca^{2+} influx from extracellular fluid through voltage-dependent calcium channels (VDCCs), receptor-operated Ca^{2+} channels, or SOCCs (27, 29). Chronic hypoxia could activate VDCCs and SOCCs through down-regulating Kv

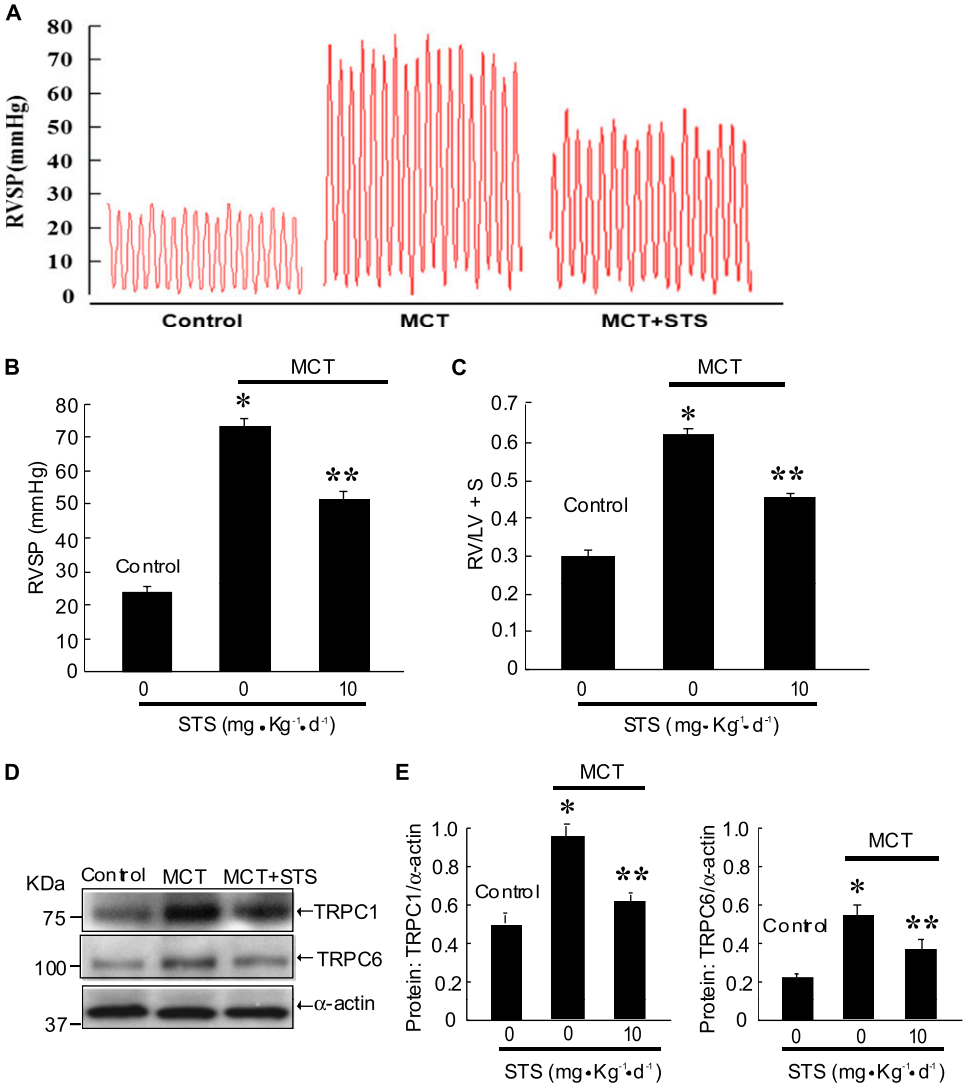

Figure 7. STS inhibited the hemodynamic parameters of PAH induced by monocrotaline (MCT) and attenuated TRPC expression in distal pulmonary arteries from rats treated with MCT. Saline- and MCT-treated animals were injected with or without STS (intraperotoneally, 10 mg/kg/d) for 21 days. (*A*) Representative traces of RVSP of each group of animals. (*B* and *C*) Bar graphs showing RVSP and RV/LV+S. Bar values are means ± SEM ($n = 6$ in each group). *$P < 0.001$ versus respective normoxic control. **$P < 0.001$ versus respective hypoxic control. (*D* and *E*) The protein levels of TRPC1 and TRPC6 were measured by Western blotting (*D*), and the intensity of their bands was normalized to that of α-actin (*E*). Data were presented as means ± SEM ($n = 4$ in each group). *$P < 0.05$ versus normoxic control. **$P < 0.05$ versus hypoxic control.

channel expression (29, 33, 41, 45–47) and up-regulates TRPC expression in PASMCs (29). Therefore, we focused on investigating the effects of STS on SOCE. Nifidepine, an antagonist of VDCCs, was included in the perfusion buffer for SOCE measurement to exclude the possibility of Ca^{2+} influx via VDCCs. In this and in our previous studies, we found that SOCE was enhanced in PASMCs from hypoxic animals (29, 30, 48). This enhancement could be blocked by STS. Thus, the inhibitory effects of STS are targeted on SOCCs but not on VDCCs.

STS might attenuate SOCE through reducing the numbers or the activity of SOCCs. The exact molecular components of SOCCs have not been fully identified. It is generally accepted that some members of the mammalian homologs of drosophila photoreceptors transient receptor potential (TRP) family (i.e., TRPC1, 4, and -6) are part of them (49). We have previously demonstrated that among the seven canonical TRP (TRPC) proteins (TRPC1–7), TRPC1, TRPC4, and TRPC6 were predominantly expressed in distal pulmonary artery and PASMCs (27, 31). Chronic or prolonged hypoxia selectively led to increases in mRNA and protein levels of TRPC1 and TRPC6 in isolated PA or cultured PASMCs (29), suggesting that TRPC1 and TRPC6 are likely the subunits of SOCCs responsible for the enhanced SOCE in PASMCs under hypoxia. Knockdown of TRPC1 or TRPC6 in PASMCs inhibited the hypoxia-induced SOCE and basal $[Ca^{2+}]_i$ up-regulation, which supported the cause–effect link between SOCE increases and TRPC expression under hypoxia (30). Therefore, we further examined whether STS affected TRPC1 and TRPC6 expression. Indeed, the STS blocked the increases of TRPC1 and TRPC6 expression in distal pulmonary arteries from hypoxic animals.

To determine whether STS exerts these inhibitory effects directly on PASMCs or due to a secondary paracrine change, PASMCs isolated from normoxic animals were cultured *in vitro* and exposed to prolonged hypoxia with or without STS. As expected, STS (12.5 and 25 μM) inhibited the hypoxia-triggered proliferation and migration of PASMCs without causing cytotoxicity. These inhibitory effects of STS under hypoxic conditions were associated with parallel molecular and functional changes, such as decreased TRPC1 and TRPC6 expression, SOCE, and basal $[Ca^{2+}]_i$ in PASMCs. Furthermore, we found that knockdown of TRPC1 or TRPC6 inhibited hypoxia-induced proliferation and migration of PASMCs, indicating a causal relationship of the hypoxic increases of PASMC proliferation and migration to increases of TRPC1 and TRPC6. Therefore, the effects of STS on basal $[Ca^{2+}]_i$ and the proliferation and migration of PASMCs are likely due to inhibited expression of TRPC1 and TRPC6.

MCT-induced PAH is another commonly used experimental model that exhibits enhanced expression of TRPC proteins in the pulmonary arterial smooth muscle (50). The above described preventive effects of STS on CHPH and its inhibitory effect

on TRPC expression may also apply to MCT-induced PAH because treatment of STS inhibited the hemodynamic parameters of PAH as well as TRPC1 and TRPC6 expression in distal PA from MCT-injected rats, indicating that a common mechanism underlies the development of the two PAH animal models.

How STS exerts inhibitory effects on TRPC expression remains to be answered. STS is a known antioxidant. It has been shown to increase intracellular production of reactive oxygen species (ROS), which in turn induce heme oxygenase-1 (HO-1) expression in macrophages, mediating the antiinflammatory effect of STS (51). STS was also found to (*1*) induce HO-1 expression in parenchymal and nonparenchymal cells in liver (52); (*2*) inhibit angiotensin II–induced cell proliferation of rat cardiac fibroblasts by interfering with ROS production and promote the eNOS-NO pathway (53); (*3*) potentiate TNF-α–mediated nuclear accumulation of Nrf2 and expression of ARE-related genes while it reversed TNF-α–induced down-regulation of intracellular glutathione, NADPH, and glucose 6-phosphate dehydrogenase levels; and (*4*) attenuate TNF-α, angiotensin II, and H_2O_2–mediated ROS production in human aortic smooth muscle cells (54). ROS was found to mediate surface expression and activation of TRPC6 channel protein in podocytes as well as vascular myocytes (55, 56). On the contrary, activation of the Nox4-ROS-PKC pathway was found to be responsible for down-regulation of TRPC6 in glomerular mesangial cells under diabetes condition (57). Hypoxia increases NOX activity and ROS production in PASMCs, and PKCε-dependent ROS-induced ROS generation is thought to play a crucial role in the hypoxic increase in $[Ca^{2+}]_i$ in PASMCs and HPV (58). In addition, AMP-activated protein kinase (AMPK) is one of the key players in maintaining intracellular homeostasis. AMPK is well known as an energy sensor and can be activated by increased cellular AMP levels. It is also known as a stress sensor and can be activated by intracellular ROS under various conditions, including exposure to hypoxia (59). Generally, the activation of AMPK turns on catabolic pathways that generate ATP while inhibiting cell proliferation and biosynthetic processes that consume ATP (59). Activation of AMPK was found to contribute to elevated $[Ca^{2+}]_i$ response to hypoxia through activation of store-operated calcium entry. STS has been shown to activate AMPK at the site of Thr(172) in human umbilical vein endothelial cells (60). The roles of ROS, PKC, and AMPK and their relationship to the inhibitory effects of STS on hypoxic up-regulation of TRPC in PASMCs remain to be determined.

In summary, this study presents essential data suggesting that the preventive effects of STS on CHPH development are at least partly due to its inhibitory actions on the expression of TRPC1 and TRPC6, the proteins that were up-regulated and responsible for altered intracellular Ca^{2+} homeostasis during the exposure to hypoxia. TRPC could also serve as a target for hypoxic pulmonary hypertension therapy. In the long history of Chinese medicine, Danshen was a low-cost herbal medicine with extensive clinical practice. The inhibitory effect of STS on elevated $[Ca^{2+}]_i$ in response to chronic hypoxia indicates a potential promising clinical application of STS on pulmonary hypertension as a cheap and effective drug. Although there is much work to be done before the final application, STS is a valuable candidate deserving further investigation for future hypoxic pulmonary hypertension therapy.

Author disclosures are available with the text of this article at www.atsjournals.org.

References

1. Galie N, Hoeper MM, Humbert M, Torbicki A, Vachiery JL, Barbera JA, Beghetti M, Corris P, Gaine S, Gibbs JS, *et al*. Guidelines for the diagnosis and treatment of pulmonary hypertension. *Eur Respir J* 2009;34:1219–1263.
2. Benza RL, Miller DP, Gomberg-Maitland M, Frantz RP, Foreman AJ, Coffey CS, Frost A, Barst RJ, Badesch DB, Elliott CG, *et al*. Predicting survival in pulmonary arterial hypertension: insights from the registry to evaluate early and long-term pulmonary arterial hypertension disease management (REVEAL). *Circulation* 2010;122:164–172.
3. Kane GC, Maradit-Kremers H, Slusser JP, Scott CG, Frantz RP, McGoon MD. Integration of clinical and hemodynamic parameters in the prediction of long-term survival in patients with pulmonary arterial hypertension. *Chest* 2011;139:1285–1293.
4. Thenappan T, Glassner C, Gomberg-Maitland M. Validation of the pulmonary hypertension connection equation for survival prediction in pulmonary arterial hypertension. *Chest* 2012;141:642–650.
5. Clements PJ, Tan M, McLaughlin VV, Oudiz RJ, Tapson VF, Channick RN, Rubin LJ, Langer A. The pulmonary arterial hypertension quality enhancement research initiative: comparison of patients with idiopathic PAH to patients with systemic sclerosis-associated PAH. *Ann Rheum Dis* 2012;71:249–252.
6. Barst RJ, Gibbs JS, Ghofrani HA, Hoeper MM, McLaughlin VV, Rubin LJ, Sitbon O, Tapson VF, Galie N. Updated evidence-based treatment algorithm in pulmonary arterial hypertension. *J Am Coll Cardiol* 2009;54(Suppl)S78–S84.
7. Kramer MR. [Combination treatment in pulmonary arterial hypertension] (in Hebrew). *Harefuah* 2011;150:383–388, 417.
8. Levinson AT, Klinger JR. Combination therapy for the treatment of pulmonary arterial hypertension. *Ther Adv Respir Dis* 2011;5:419–430.
9. Abraham T, Wu G, Vastey F, Rapp J, Saad N, Balmir E. Role of combination therapy in the treatment of pulmonary arterial hypertension. *Pharmacotherapy* 2010;30:390–404.
10. Kahler CM. [Combination therapy for the treatment of pulmonary arterial hypertension] (in German). *Dtsch Med Wochenschr* 2009;134: S181–S182.
11. Benza RL, Rayburn BK, Tallaj JA, Pamboukian SV, Bourge RC. Treprostinil-based therapy in the treatment of moderate-to-severe pulmonary arterial hypertension: long-term efficacy and combination with bosentan. *Chest* 2008;134:139–145.
12. Jiang WD, Yu YZ, Liu WW, Chen YH, Wang YP, Huang TC. [Effects of sodium tanshinone II-A sulfonate and propranolol on coronary collaterals in acutely infarcted dogs] (in Chinese). *Zhongguo Yao Li Xue Bao* 1981;2:29–33.
13. Liu J, Morton J, Miedzyblocki M, Lee TF, Bigam DL, Fok TF, Chen C, Lee SK, Davidge ST, Cheung PY. Sodium tanshinone IIA sulfonate increased intestinal hemodynamics without systemic circulatory changes in healthy newborn piglets. *Am J Physiol Heart Circ Physiol* 2009;297:H1217–H1224.
14. Zhou L, Zuo Z, Chow MS. Danshen: an overview of its chemistry, pharmacology, pharmacokinetics, and clinical use. *J Clin Pharmacol* 2005;45:1345–1359.
15. Feng J, Zheng Z. Effect of sodium tanshinone II A sulfonate on cardiac myocyte hypertrophy and its underlying mechanism. *Chin J Integr Med* 2008;14:197–201.
16. Zhou D, Liang Q, He X, Zhan C. Changes of c-Fos and c-jun mRNA expression in angiotensin II–induced cardiomyocyte hypertrophy and effects of sodium tanshinone IIA sulfonate. *J Huazhong Univ Sci Technolog Med Sci* 2008;28:531–534.
17. Yang Y, Cai F, Li PY, Li ML, Chen J, Chen GL, Liu ZF, Zeng XR. Activation of high conductance Ca(2+)-activated K(+) channels by sodium tanshinone II-A sulfonate (ds-201) in porcine coronary artery smooth muscle cells. *Eur J Pharmacol* 2008;598:9–15.
18. Gao S, Liu Z, Li H, Little PJ, Liu P, Xu S. Cardiovascular actions and therapeutic potential of tanshinone IIA. *Atherosclerosis* 2012;220:3–10.
19. Huang YF, Liu ML, Dong MQ, Yang WC, Zhang B, Luan LL, Dong HY, Xu M, Wang YX, Liu LL, *et al*. Effects of sodium tanshinone II A sulphonate on hypoxic pulmonary hypertension in rats *in vivo* and on Kv2.1 expression in pulmonary artery smooth muscle cells *in vitro*. *J Ethnopharmacol* 2009;125:436–443.
20. Wang J, Dong MQ, Liu ML, Xu DQ, Luo Y, Zhang B, Liu LL, Xu M, Zhao PT, Gao YQ, *et al*. Tanshinone IIA modulates pulmonary vascular response to agonist and hypoxia primarily via inhibiting Ca2+ influx and release in normal and hypoxic pulmonary hypertension rats. *Eur J Pharmacol* 2010;640:129–138.
21. Leach RM, Treacher DF. Clinical aspects of hypoxic pulmonary vasoconstriction. *Exp Physiol* 1995;80:865–875.

22. Stenmark KR, Fagan KA, Frid MG. Hypoxia-induced pulmonary vascular remodeling: cellular and molecular mechanisms. *Circ Res* 2006; 99:675–691.
23. Hanasato N, Oka M, Muramatsu M, Nishino M, Adachi H, Fukuchi Y. E-4010, a selective phosphodiesterase 5 inhibitor, attenuates hypoxic pulmonary hypertension in rats. *Am J Physiol* 1999;277:L225–L232.
24. Oka M, Morris KG, McMurtry IF. NIP-121 is more effective than Nifedipine in acutely reversing chronic pulmonary hypertension. *J Appl Physiol* 1993;75:1075–1080.
25. Muramatsu M, Oka M, Morio Y, Soma S, Takahashi H, Fukuchi Y. Chronic hypoxia augments endothelin-B receptor-mediated vasodilation in isolated perfused rat lungs. *Am J Physiol* 1999;276:L358–L364.
26. Liu X, Singh BB, Ambudkar IS. TRPC1 is required for functional store-operated Ca2+ channels: role of acidic amino acid residues in the s5-s6 region. *J Biol Chem* 2003;278:11337–11343.
27. Wang J, Shimoda LA, Sylvester JT. Capacitative calcium entry and TRPC channel proteins are expressed in rat distal pulmonary arterial smooth muscle. *Am J Physiol Lung Cell Mol Physiol* 2004;286:L848–L858.
28. Wang J, Semenza G, Sylvester JT, Shimoda LA. Hif-1 regulates hypoxic-induction of canonical transient receptor potential (TRPC) channels in pulmonary arterial smooth muscle cells [abstract]. *FASEB J* 2005; 19:A1278.
29. Wang J, Weigand L, Lu W, Sylvester JT, Semenza GL, Shimoda LA. Hypoxia inducible factor 1 mediates hypoxia-induced TRPC expression and elevated intracellular Ca2+ in pulmonary arterial smooth muscle cells. *Circ Res* 2006;98:1528–1537.
30. Lu W, Ran P, Zhang D, Peng G, Li B, Zhong N, Wang J. Sildenafil inhibits chronically hypoxic upregulation of canonical transient receptor potential expression in rat pulmonary arterial smooth muscle. *Am J Physiol Cell Physiol* 2009;298:C114–C123.
31. Lu W, Wang J, Shimoda LA, Sylvester JT. Differences in STIM1 and TRPC expression in proximal and distal pulmonary arterial smooth muscle are associated with differences in Ca2+ responses to hypoxia. *Am J Physiol Lung Cell Mol Physiol* 2008;295:L104–L113.
32. Shimoda LA, Sham JS, Sylvester JT. Altered pulmonary vasoreactivity in the chronically hypoxic lung. *Physiol Res* 2000;49:549–560.
33. Lu W, Ran P, Zhang D, Lai N, Zhong N, Wang J. Bone morphogenetic protein 4 enhances canonical transient receptor potential expression, store-operated Ca2+ entry, and basal [Ca2+]i in rat distal pulmonary arterial smooth muscle cells. *Am J Physiol Cell Physiol* 2010;299: C1370–C1378.
34. Lu W, Wang J, Peng G, Shimoda LA, Sylvester JT. Knockdown of stromal interaction molecule 1 attenuates store-operated Ca2+ entry and Ca2+ responses to acute hypoxia in pulmonary arterial smooth muscle. *Am J Physiol Lung Cell Mol Physiol* 2009;297:L17–L25.
35. Lu HZ, Hu JG. Expression of bone morphogenetic proteins-2/4 in neural stem cells and their lineages. *Acta Neurobiol Exp (Warsz)* 2009;69: 441–447.
36. Nong Z, Stassen JM, Moons L, Collen D, Janssens S. Inhibition of tissue angiotensin-converting enzyme with quinapril reduces hypoxic pulmonary hypertension and pulmonary vascular remodeling. *Circulation* 1996;94:1941–1947.
37. Adamy C, Oliviero P, Eddahibi S, Rappaport L, Samuel JL, Teiger E, Chassagne C. Cardiac modulations of ANG II receptor expression in rats with hypoxic pulmonary hypertension. *Am J Physiol Heart Circ Physiol* 2002;283:H733–H740.
38. Sun D, Shen M, Li J, Li W, Zhang Y, Zhao L, Zhang Z, Yuan Y, Wang H, Cao F. Cardioprotective effects of tanshinone IIA pretreatment via kinin b2 receptor-AKT-GSK-3beta dependent pathway in experimental diabetic cardiomyopathy. *Cardiovasc Diabetol* 2011;10:4.
39. Wang P, Wu X, Bao Y, Fang J, Zhou S, Gao J, Pi R, Mou YG, Liu P. Tanshinone IIA prevents cardiac remodeling through attenuating NAD(P)H oxidase-derived reactive oxygen species production in hypertensive rats. *Pharmazie* 2011;66:517–524.
40. Xu W, Yang J, Wu LM. Cardioprotective effects of tanshinone IIA on myocardial ischemia injury in rats. *Pharmazie* 2009;64:332–336.
41. Rodman DM. Chronic hypoxia selectively augments rat pulmonary artery Ca^{2+} and K^+ channel-mediated relaxation. *Am J Physiol* 1992; 263:L88–L94.
42. Mandegar M, Fung YC, Huang W, Remillard CV, Rubin LJ, Yuan JX. Cellular and molecular mechanisms of pulmonary vascular remodeling: role in the development of pulmonary hypertension. *Microvasc Res* 2004;68:75–103.
43. Stanbrook HS, Morris KG, McMurtry IF. Prevention and reversal of hypoxic pulmonary hypertension by calcium antagonists. *Am Rev Respir Dis* 1984;130:81–85.
44. Platoshyn O, Golovina VA, Bailey CL, Limsuwan A, Krick S, Juhaszova M, Seiden JE, Rubin LJ, Yuan JX. Sustained membrane depolarization and pulmonary artery smooth muscle cell proliferation. *Am J Physiol Cell Physiol* 2000;279:C1540–C1549.
45. Wang J, Juhaszova M, Rubin LJ, Yuan XJ. Hypoxia inhibits gene expression of voltage-gated K^+ channel alpha subunits in pulmonary artery smooth muscle cells. *J Clin Invest* 1997;100:2347–2353.
46. Liu JQ, Sham JS, Shimoda LA, Kuppusamy P, Sylvester JT. Hypoxic constriction and reactive oxygen species in porcine distal pulmonary arteries. *Am J Physiol Lung Cell Mol Physiol* 2003;285:L322–L333.
47. Wang J, Weigand L, Wang W, Sylvester JT, Shimoda LA. Chronic hypoxia inhibits K_v channel gene expression in rat distal pulmonary artery. *Am J Physiol Lung Cell Mol Physiol* 2005;288:L1049–L1058.
48. Wang J, Shimoda LA, Weigand L, Wang W, Sun D, Sylvester JT. Acute hypoxia increases intracellular $[Ca^{2+}]$ in pulmonary arterial smooth muscle by enhancing capacitative Ca^{2+} entry. *Am J Physiol Lung Cell Mol Physiol* 2005;288:L1059–L1069.
49. Cook B, Minke B. Trp and calcium stores in *Drosophila* phototransduction. *Cell Calcium* 1999;25:161–171.
50. Liu XR, Zhang MF, Yang N, Liu Q, Wang RX, Cao YN, Yang XR, Sham JS, Lin MJ. Enhanced store-operated Ca2+ entry and TRPC channel expression in pulmonary arteries of monocrotaline-induced pulmonary hypertensive rats. *Am J Physiol Cell Physiol* 2012;302: C77–C87.
51. Chen TH, Hsu YT, Chen CH, Kao SH, Lee HM. Tanshinone IIA from *Salvia miltiorrhiza* induces heme oxygenase-1 expression and inhibits lipopolysaccharide-induced nitric oxide expression in Raw 264.7 cells. *Mitochondrion* 2007;7:101–105.
52. Qi YY, Xiao L, Zhang LD, Song SH, Mei Y, Chen T, Tang JM, Liu F, Ding GS, Shi YZ, *et al*. Tanshinone IIA pretreatment attenuates hepatic ischemia-reperfusion. *Front Biosci* 2012;4:1303–1313. (Elite Ed).
53. Chan P, Liu JC, Lin LJ, Chen PY, Cheng TH, Lin JG, Hong HJ. Tanshinone iia inhibits angiotensin II–induced cell proliferation in rat cardiac fibroblasts. *Am J Chin Med* 2011;39:381–394.
54. Zhang HS, Wang SQ. Nrf2 is involved in the effect of tanshinone IIA on intracellular redox status in human aortic smooth muscle cells. *Biochem Pharmacol* 2007;73:1358–1366.
55. Kim EY, Anderson M, Dryer SE. Insulin increases surface expression of TRPC6 channels in podocytes: role of NADPH oxidases and reactive oxygen species. *Am J Physiol Renal Physiol* 2012;302:F298–F307.
56. Ding Y, Winters A, Ding M, Graham S, Akopova I, Muallem S, Wang Y, Hong JH, Gryczynski Z, Yang SH, *et al*. Reactive oxygen species-mediated TRPC6 protein activation in vascular myocytes, a mechanism for vasoconstrictor-regulated vascular tone. *J Biol Chem* 2011; 286:31799–31809.
57. Graham S, Gorin Y, Abboud HE, Ding M, Lee DY, Shi H, Ding Y, Ma R. Abundance of TRPC6 protein in glomerular mesangial cells is decreased by ROS and PKC in diabetes. *Am J Physiol Cell Physiol* 2011;301:C304–C315.
58. Rathore R, Zheng YM, Niu CF, Liu QH, Korde A, Ho YS, Wang YX. Hypoxia activates NADPH oxidase to increase [ROS]i and [Ca2+]i through the mitochondrial ROS-PKCepsilon signaling axis in pulmonary artery smooth muscle cells. *Free Radic Biol Med* 2008;45: 1223–1231.
59. Wang S, Song P, Zou MH. Amp-activated protein kinase, stress responses and cardiovascular diseases. *Clin Sci (Lond)* 2012;122: 555–573.
60. Pan C, Lou L, Huo Y, Singh G, Chen M, Zhang D, Wu A, Zhao M, Wang S, Li J. Salvianolic acid b and tanshinone IIA attenuate myocardial ischemia injury in mice by no production through multiple pathways. *Ther Adv Cardiovasc Dis* 2011;5:99–111.